Received: 16 December 2025 | Revised: 01 January 2026 | Accepted: 04 February 2026
DOI: 10.48309/JMPCR.2026.566559.1943
Journal of Medicinal and Pharmaceutical Chemistry Research
SAMI

FULL PAPER

Computational investigation of *Cissus quadrangularis* phytoconstituents as aryl hydrocarbon receptor modulators for psoriasis therapy

Konatham Teja Kumar Reddy[1] | Mobeen Shaik[2] | Karthickeyan Krishnan[3,*] | Phanindra Erukulla[4] | Pericharla Venkata Narasimha Raju[5] | T. Siva Krishna[6] | Mohit Kumar[7] | CH K V L S N Anjana Male[8,*]

[1]*Department of Pharmaceutical Analysis, Malla Reddy Institute of Pharmaceutical Sciences, Malla Reddy Vishwavidyapeeth (Deemed to be University), Secunderabad, 500100, Telangana, India*

[2]*Department of Pharmaceutics, KL College of Pharmacy, Koneru Lakshmaiah Education Foundation (Deemed to be University), Guntur Andhra Pradesh, India*

[3]*Department of Pharmacy Practice, School of Pharmaceutical Sciences, Vels Institute of Science, Technology and Advanced Studies (VISTAS), Pallavaram, Chennai 600 117, India*

[4]*Department of Regulatory Affairs, Ricon Pharma LLC, 100 Ford Rd, Suite #9, Denville, NJ 07834, United state*

[5]*Department of Regulatory Affairs, Hikma Pharmaceuticals USA Inc.,2 Esterbrook Lane, Cherry Hill, NJ 08003, United state*

[6]*Department of Mathematics Ramachandra College of Engineering, Eluru, Andhra Pradesh, India*

[7]*Teerthanker Mahaveer College of Pharmacy, Teerthanker Mahaveer University, Moradabad, Uttar Pradesh, India*

[8]*School of Pharmacy ITM University, Jhansi Rd, Turari, Gwalior, Lakhnotikhurd, Madhya Pradesh 474001, India*

***Corresponding Author:**
Karthickeyan Krishnan
E-mail: karthickeyanpharmacy@gmail.com
CH K V L S N Anjana Male
E-mail: anjana.male@gmail.com
Tel.: 628126026930

Psoriasis is a chronic inflammatory skin disorder in which dysregulation of the aryl hydrocarbon receptor (AhR) contributes significantly to keratinocyte hyperproliferation and immune imbalance. In this study, a comprehensive computational investigation was conducted to evaluate the phytoconstituents of *Cissus quadrangularis* as potential AhR modulators. Sixteen bioactive compounds were screened through molecular docking against AhR (PDB ID: 7ZUB) and the binding interactions were compared with those of the native ligand. The docking analysis revealed that several phytochemicals exhibited stronger affinities than the native ligand, with quercetin-3-O-α-L-rhamnopyranoside (–10.4 kcal/mol), β-sitosterol acetate (–10.3 kcal/mol), cholesterin (–9.4 kcal/mol), and β-amyrone (–9.0 kcal/mol) emerging as the most potent candidates. These molecules demonstrated extensive hydrogen bonding, π-cation interactions, and hydrophobic stabilization, indicating their high compatibility with the AhR-binding pocket. The top-performing compounds were subsequently subjected to ADMET evaluation to assess their pharmacokinetic behavior and safety. The predicted physicochemical parameters indicated a broad logP range (1.31–8.34) and TPSA values spanning 17.07–190.28 Å^2, reflecting diverse permeability and solubility characteristics. Several candidates demonstrated improved drug-likeness, favorable metabolic stability, and reduced predicted carcinogenicity compared with the native ligand. Notably, quercetin-3-O-α-L-rhamnopyranoside and diphenyl sulfone exhibited balanced ADMET properties, whereas lipophilic triterpenoids showed enhanced distribution potential. These results support the therapeutic potential of *Cissus quadrangularis* phytoconstituents and provide a strong foundation for future *in vitro* and *in vivo* validation of psoriasis management.

KEYWORDS

Cissus quadrangularis; aryl hydrocarbon receptor; computational investigation; psoriasis; phytoconstituents; drug discovery.

Introduction

Psoriasis is a chronic immune-mediated dermatological disorder characterized by keratinocyte hyperproliferation, aberrant differentiation, and persistent inflammation. The global prevalence of psoriasis continues to rise, placing a significant burden on patients' physical, psychological, and socioeconomic well-being. Although several therapeutic strategies, such as corticosteroids, vitamin D analogs, phototherapy, and biologics, are currently available, they remain limited by

high costs, adverse effects, variable patient responsiveness, and the need for long-term management. These challenges highlight the need for novel, safer, and more accessible therapeutic alternatives, particularly those derived from natural products with established traditional medicinal uses [1–4]. Recent advances in molecular pharmacology have identified the AhR as a promising therapeutic target in psoriasis. AhR is a ligand-activated transcription factor that regulates epidermal homeostasis, immune response, and xenobiotic metabolism. Dysregulated AhR signaling contributes to abnormal keratinocyte proliferation and inflammatory cytokine production, both of which are central to psoriasis pathogenesis. Selective modulation of AhR activity has shown potential for restoring epidermal function and attenuating psoriatic inflammation, making AhR ligands attractive candidates for therapeutic development [5–9].

Cissus quadrangularis, a medicinal plant widely used in Ayurveda and traditional African medicine, is rich in phytoconstituents such as flavonoids, sterols, triterpenoids, and phenolic compounds. These bioactive molecules have demonstrated antioxidant, anti-inflammatory, antimicrobial, and wound healing activities, suggesting their potential relevance in managing dermatological conditions, including psoriasis [10–13]. However, the molecular mechanisms underlying their therapeutic actions, particularly their ability to modulate AhR, remain largely unexplored. Computational approaches, including molecular docking and ADMET (Absorption, Distribution, Metabolism, Excretion, and Toxicity) modeling, provide a rapid and cost-effective platform for screening large numbers of phytochemicals and predicting their pharmacological behavior. Molecular docking facilitates the identification of compounds with strong binding affinities and favorable interactions with target proteins, such as AhR. Complementary ADMET analysis ensures that the most promising candidates exhibit adequate drug-likeness, pharmacokinetic suitability, and safety profiles before experimental validation. Integrating these computational tools accelerates the early stages of drug discovery and enables rational selection of phytoconstituents with the highest therapeutic potential [14–17].

Several medicinal plants, including Indigofera tinctoria, Curcuma longa, and Artemisia species, have been reported to influence AhR signaling through bioactive polyphenols, indole derivatives, and sesquiterpenes. Although these plants demonstrate AhR-modulating potential, many are characterized by relatively narrow phytochemical diversity or have been extensively investigated with respect to AhR-associated pathways. In contrast, *Cissus quadrangularis* possesses a broad spectrum of flavonoids, sterols, triterpenoids, and phenolic compounds with established anti-inflammatory and dermatological relevance; however, its interaction with AhR remains largely unexplored. This unique phytochemical complexity, together with its long-standing traditional use in skin and inflammatory disorders, provides a compelling rationale for selecting *Cissus quadrangularis* for AhR-targeted computational investigation in psoriasis therapy [18–20].

Given these considerations, the present study aimed to perform a comprehensive computational investigation of the major phytoconstituents of *Cissus quadrangularis* to evaluate their potential as AhR modulators for psoriasis management. By employing molecular docking to elucidate receptor–ligand interactions and ADMET modeling to assess pharmacokinetic feasibility, this study sought to identify plant-derived compounds with favorable biological and drug development attributes. This approach contributes to the growing interest in natural product-based therapeutics and offers scientific insight into the molecular basis of the traditional use of *Cissus quadrangularis* in skin health and inflammatory disorders.

Experimental Section

Selection of compounds

The selection of phytoconstituents for this study was informed by published phytochemical investigations of *Cissus quadrangularis*, supported by GC–MS and LC–MS profiling documented in recent literature. Multiple reports have confirmed that *Cissus* quadrangularis contains a diverse spectrum of secondary metabolites including sterols, triterpenoids, fatty acids, flavonoids, phenolics, terpenoids, aldehydes, and heterocyclic compounds, many of which have demonstrated biological activities relevant to inflammatory and dermatological disorders. Furthermore, LC–MS data from ethanolic extracts identified several key constituents, such as β-amyrone, β-sitosterol acetate, cholesterin, carotene, "quinoline, 1,2-dihydro-2,2,4-trimethyl," quinoline, tetradecanoic acid, quercetin-3-O-α-L-rhamnopyranoside, and linoleic acid, confirming their natural occurrence in the plant [21]. Several of these compounds, such as 13-docosenamide, diphenyl sulfone, neophytadiene, and sterol derivatives, have been previously identified as dominant GC–MS peaks in C. quadrangularis extracts, supporting their relevance for inclusion in this study [22]. Based on these phytochemical profiles, 16 representative compounds were selected for the computational screening. This selection captured the major chemical classes reported in literature, as shown in Figure 1. The chemical structures of all 16 phytoconstituents were retrieved from the PubChem database and cross-verified with the literature-reported structures to ensure accuracy. Ligands were subsequently cleaned, energy minimized, and converted into appropriate formats for molecular docking analysis following standard ligand-preparation workflows, similar to those described in recent *Cissus quadrangularis in silico* investigations. This literature-driven selection ensured broad phytochemical coverage and biological relevance, forming a robust foundation for subsequent molecular docking and ADMET evaluation to identify potential AhR modulators for psoriasis therapy.

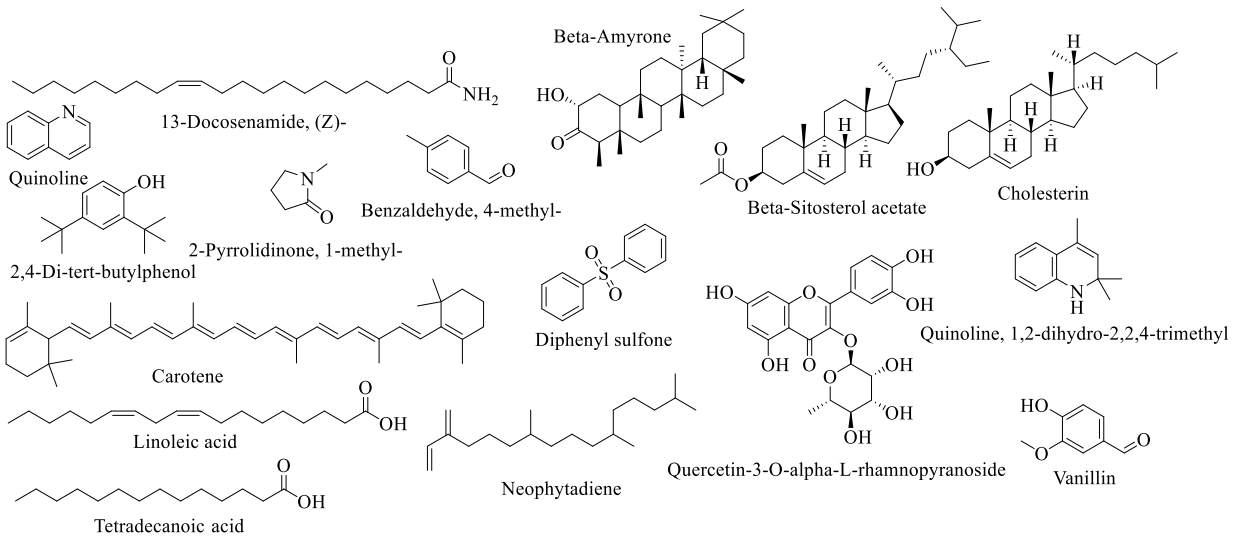

FIGURE 1 Chemical structures of all selected compounds

Molecular docking

Molecular docking was performed to evaluate the binding affinities and interaction profiles of *Cissus quadrangularis* phytoconstituents with AhR using a structure-based virtual screening approach. The three-dimensional structure of AhR (PDB ID: 7ZUB) was retrieved from the RCSB Protein Data Bank to be used as a target receptor (Figure 2). Prior to docking, the receptor structure was prepared using Discovery Studio by removing crystallographic water molecules, correcting missing residues, and adding polar hydrogen atoms to stabilize the protein [23]. The active site region was defined based on the reported ligand-binding domain, and the docking grid was centered using the following XYZ coordinates: X = 166.996385, Y = 129.239128, and Z = 201.742923, which ensured optimal coverage of the receptor's functional pocket.

The selected ligands were first sketched and optimized using ChemDraw, and their corresponding 3D structures were obtained from PubChem, where necessary. All ligand structures were energy-minimized and converted to the PDBQT format using PyRx (Version 0.9), which employs the Open Babel module for geometry optimization and force field minimization. Each compound underwent preparation steps, including hydrogen addition, charge assignment, and conversion to low-energy conformers suitable for molecular docking. Docking simulations were performed using AutoDock Vina, integrated with the PyRx platform. A Lamarckian Genetic Algorithm-based search was applied to explore ligand conformations within the defined grid box. The exhaustiveness parameters were maintained at default settings to ensure a balance between the computational cost and search accuracy. Multiple poses were generated for each ligand, and the pose with the lowest binding energy (kcal/mol) was selected as the most favorable conformation. Post-docking analysis was carried out using Discovery Studio Visualizer, where receptor–ligand complexes were examined for hydrogen bonds, hydrophobic contacts, π-interactions, electrostatic forces, and other stabilizing interactions [24–26]. The binding modes were compared with those of the native ligand to assess the potential of each phytoconstituent as an AhR modulator. This systematic docking workflow enabled the reliable identification of phytochemicals with strong affinity and favorable interaction profiles toward AhR, supporting their further evaluation in ADMET and pharmacokinetic analyses.

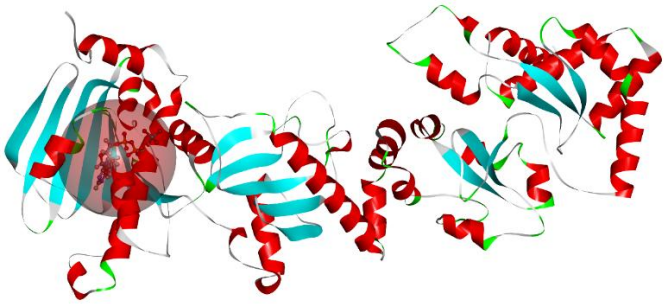

FIGURE 2 Active cavity of AhR with native ligand

ADMET evaluation

The pharmacokinetic and toxicity profiles of the selected phytoconstituents were assessed using systematic ADMET analysis to determine their suitability as potential AhR modulators. This evaluation was conducted using a combination of structure preparation tools and computational prediction platforms. Initially, all the ligand structures were drawn and refined using ChemDraw to ensure proper

stereochemistry, valency, and structural accuracy. The final structures were cross-validated with the corresponding entries in the PubChem database, from which canonical SMILES and SDF files were retrieved for computational processing. These standardized formats were used as inputs to maintain consistency across predictive models. The ADMET properties of each compound were predicted using ADMETlab 3.0, an advanced web-based platform that integrates machine learning and quantitative structure–activity relationship (QSAR) algorithms. The evaluated parameters included physicochemical descriptors (molecular weight, topological polar surface area (TPSA), hydrogen bond donors/acceptors), drug-likeness metrics (Lipinski rule, Pfizer rule, GSK rule, Golden Triangle), absorption indicators (Caco-2 permeability, MDCK permeability, P-gp affinity, and human intestinal absorption), distribution properties (plasma protein binding, volume of distribution, blood–brain barrier penetration), metabolic interactions (CYP450 inhibition and substrate potential), excretion rates, and toxicity endpoints (hepatotoxicity, carcinogenicity, Ames mutagenicity, skin sensitization, and organ-specific toxicity). The predicted values of each compound were recorded and compared with those of the native ligand to identify molecules with superior pharmacokinetic behavior and minimal toxicity risk [16,27,28]. This multi-layered computational evaluation enabled the early identification of phytoconstituents with optimal ADMET performance, thereby supporting their potential progression as drug-like AhR modulators.

Results and Discussion

Molecular docking

Molecular docking analysis revealed a diverse range of interaction profiles between AhR and phytoconstituents from *Cissus quadrangularis*, highlighting several promising modulators with strong binding affinities (Table 1). 2D and 3D interaction poses with AhR are shown in Figure 3. The native ligand exhibited the most extensive interaction network, including attractive electrostatic contacts with GLU42 and multiple hydrogen bonds involving ASN46, GLY109, THR110, GLN128, and PHE129, resulting in a favorable docking score of –9.6 kcal/mol. This high-affinity binding serves as a benchmark for the evaluation of phytochemicals. Among the tested constituents, Quercetin-3-O-α-L-rhamnopyranoside demonstrated the strongest binding affinity (–10.4 kcal/mol), surpassing that of the native ligand. Its interaction profile includes several conventional hydrogen bonds with THR110, LYS107, ASP88, ASN46, and SER108, accompanied by electrostatic π-cation interactions with LYS53 and hydrophobic π-alkyl contacts with MET93 and other residues. The richness of the binding interactions suggests an exceptional complementarity with the AhR active site. β-Sitosterol acetate also displayed strong affinity (–10.3 kcal/mol), forming hydrogen bonds with GLN128, PHE129, GLY130, VAL131, GLY132, and ARG392, supported by hydrophobic interactions with MET93, LYS53, ILE91, and PHE113. The combination of polar and hydrophobic contacts enhances receptor stabilization, making it a key candidate for AhR modulation. Other compounds with notable docking scores included cholesterin (–9.4 kcal/mol), β-amyrone (–9.0 kcal/mol), and carotene (–8.3 kcal/mol), all of which predominantly engaged in alkyl and π-alkyl hydrophobic interactions. These interactions suggest suitability for stabilizing hydrophobic pockets within AhR, but with fewer directional bonds than glycosylated flavonoids. Moderately active ligands such as 2,4-di-tert-butylphenol (–6.5 kcal/mol), quinoline derivatives (–6.4 to –6.1 kcal/mol), linoleic acid (–6.1 kcal/mol), and vanillin (–6.1 kcal/mol) formed fewer hydrogen bonds and mainly hydrophobic contacts, resulting in

lower affinity. Compounds like 2-pyrrolidinone (–4.2 kcal/mol) and neophytadiene (–5.8 kcal/mol) showed limited interaction strength and fewer molecular contacts, indicating a weaker capability to modulate AhR. Overall, the docking results clearly indicated that quercetin-3-O-α-L-rhamnopyranoside, β-sitosterol acetate, cholesterin, and β-amyrone exhibited strong binding potentials comparable to or exceeding that of the native ligand. The presence of multiple hydrogen bonds, π-interactions, and hydrophobic stabilization contributes to their favorable receptor affinity, suggesting their potential as effective AhR modulators for psoriasis therapy.

TABLE 1 Binding interactions of selected compounds with AhR

Amino acid	Bond length	Bond type	Bond category	Ligand energy (Kcal/mol)	Docking score
Native ligand					
GLU42	5.53091	Electrostatic	Attractive Charge		
GLU42	4.16045				
ASN46	2.63571				
GLY109	2.71065				
THR110	2.42316				
GLN128	2.69766				
PHE129	3.00172				
PHE129	2.23438	Hydrogen Bond	Conventional Hydrogen Bond	1509.92	-9.6
GLY130	2.1974				
VAL131	2.77879				
VAL131	2.61055				
GLY132	2.06668				
GLY132	2.50704				
ARG392	2.66585				
ARG392	2.61267				
GLY127	3.31587		Carbon Hydrogen Bond		
2,4-Di-tert-butylphenol					
ASN46	3.98177	Hydrophobic	Pi-Sigma	93.87	-6.5
LEU102	5.40897				
VAL181	5.29796		Alkyl		
ALA50	4.30184				
ALA50	4.56294		Pi-Alkyl		
PHE133	4.89232				
2-Pyrrolidinone, _1-methyl-					
GLY109	2.47772	Hydrogen Bond	Conventional Hydrogen Bond	70.48	-4.2
THR110	2.10395				
ASN46	3.73307		Carbon Hydrogen Bond		
13-Docosenamide, _(Z)-					
GLY127	3.02447	Hydrogen Bond	Conventional Hydrogen Bond	78.1	-6.1
SER108	2.30624				
PHE129	2.62183				

Amino acid	Bond length	Bond type	Bond category	Ligand energy (Kcal/mol)	Docking score
			Native ligand		
GLY130	2.10654				
			Benzaldehyde, _4-methyl-		
SER108	2.35588	Hydrogen Bond	Conventional Hydrogen Bond	49.47	-5.3
PHE129	2.66044				
GLY130	2.17075				
VAL131	4.19058		Amide-Pi Stacked		
LEU102	4.82746	Hydrophobic	Alkyl		
PHE133	5.45878		Pi-Alkyl		
			B-Amyrone		
ILE91	5.04741	Hydrophobic	Alkyl	585.87	-9
MET93	3.85229				
ALA112	4.24851				
LYS53	4.13148				
NILE91	3.60523				
MET93	3.80512				
ALA50	4.4912				
LYS53	4.28382				
ILE91	4.88658				
MET93	5.48306				
ALA50	5.33567				
MET93	4.13687				
PHE113	5.37288		Pi-Alkyl		
PHE11	5.38327				
			Beta-Sitosterol_acetate		
GLN128	2.62759	Hydrogen Bond	Conventional Hydrogen Bond	475.65	-10.3
PHE129	2.10749				
GLY130	2.38935				
VAL131	2.53462				
GLY132	2.17527				
ARG392	2.95632				
ARG392	2.81655				
MET93	3.34825				
LYS53	4.20253				
ILE91	4.18044	Hydrophobic	Alkyl		
ILE91	4.02983				
ALA50	4.11689				
PHE113	4.74175		Pi-Alkyl		
HIS149	4.58699				
			Carotene		
ALA112	3.67307	Hydrophobic	Alkyl	241.34	-8.3
LYS53	5.09416				
ILE91	4.07702				

Amino acid	Bond length	Bond type	Bond category	Ligand energy (Kcal/mol)	Docking score
			Native ligand		
ALA50	3.77591				
LEU102	4.26583				
VAL145	4.1316				
VAL181	4.96102				
LEU102	5.41266				
VAL181	4.79773				
PHE113	5.0845				
PHE133	4.46301		Pi-Alkyl		
PHE133	4.6667				
			Cholesterin		
VAL181	5.47707				
LEU102	5.38897				
VAL145	4.65618				
VAL181	4.68101	Hydrophobic	Alkyl	388.54	-9.4
MET93	4.6192				
LEU102	4.42421				
ALA50	5.01773				
PHE133	5.21889		Pi-Alkyl		
			Diphenyl_sulfone		
SER108	2.95429				
GLY109	2.1726	Hydrogen Bond	Conventional Hydrogen Bond	422.24	-7
GLY109	2.43772				
THR110	2.16182				
LYS53	3.63602	Electrostatic	Pi-Cation		
ALA50	5.40478	Hydrophobic	Pi-Alkyl		
			Linoleic_acid		
GLY132	2.59085	Hydrogen Bond	Conventional Hydrogen Bond		
PHE133	2.14732				
LEU102	4.85271	Hydrophobic	Alkyl	1.69	-6.1
VAL145	4.66483				
VAL181	4.97299				
PHE133	4.8782		Pi-Alkyl		
			Neophytadiene		
MET93	4.75574				
LEU102	4.64767				
LEU102	4.46596				
VAL145	3.97947		Alkyl		
VAL181	4.68759	Hydrophobic		46.49	-5.8
ALA50	3.84537				
MET93	3.62316				
PHE133	5.17923		Pi-Alkyl		
PHE133	4.50268				

Amino acid	Bond length	Bond type	Bond category	Ligand energy (Kcal/mol)	Docking score
Native ligand					
TYR134	4.48895				
Quercetin-3-O-α-L-rhamnopyranoside					
THR110:OG1	2.9169				
LYS107	2.05905	Hydrogen Bond	Conventional Hydrogen Bond		
ASP88	1.92123				
ASN46	2.93174				
SER108	2.75027				
LYS53	3.91297	Electrostatic	Pi-Cation	781.25	-10.4
ALA47	4.97536		Amide-Pi Stacked		
ASN46	4.33439				
MET93	5.43561				
ALA47	5.29929	Hydrophobic			
VAL181	5.41184		Pi-Alkyl		
ALA50	4.94936				
MET93	4.44488				
Quinoline, 1,2-dihydro-2,2,4-trimethyl					
ASP88	2.24167	Hydrogen Bond	Conventional Hydrogen Bond		
THR179	3.08053		Pi-Donor Hydrogen Bond		
LEU102	4.87724		Alkyl	884.24	-6.4
ALA50	4.3435	Hydrophobic			
MET93	5.07871		Pi-Alkyl		
PHE133	4.47287				
Quinoline					
ASP88	2.05192	Hydrogen Bond	Conventional Hydrogen Bond		
VAL181	3.84348		Pi-Sigma		
ALA50	4.92728	Hydrophobic	Alkyl	88.77	-6.1
LEU43	5.29587		Pi-Alkyl		
ALA47	5.30319				
Tetradecanoic_acid					
ASN46	2.70615				
ASN46	2.2202	Hydrogen Bond	Conventional Hydrogen Bond		
GLY132	2.52004			3.05	-5.6
PHE133	2.29506				
ALA50	3.67969	Hydrophobic	Alkyl		
Vanillin					
GLY130	3.06232				
SER108	2.61881				
GLY109	2.49241	Hydrogen Bond	Conventional Hydrogen Bond	77.33	-6.1
THR110	2.12465				
GLY132	2.61604				

Amino acid	Bond length	Bond type	Bond category	Ligand energy (Kcal/mol)	Docking score
			Native ligand		
GLY132	3.02161				
PHE133	2.69904				
PHE133	2.13767				
ASN46	3.3838		Carbon Hydrogen Bond		

ADMET evaluation

Based on insights derived from the molecular docking results, the seven most potent phytocompounds selected for their superior binding affinities and interaction profiles with AhR were subjected to extensive ADMET evaluation. This multistep assessment aimed to characterize the physicochemical suitability, drug-likeness, absorption behavior, distribution potential, metabolic stability, excretion patterns, and toxicity risks of each compound. By comparing these parameters with those of the native ligand, this study sought to determine the relative pharmacokinetic advantages and potential safety considerations associated with each derivative. This combined analysis provides a robust framework for identifying promising AhR modulators with improved therapeutic prospects. Physicochemical evaluation revealed considerable variation among the selected derivatives when compared with the native ligand (Table 2). The native molecule displayed high polarity (TPSA 232.6 Å^2) and a negative logP value (–2.67), indicating hydrophilicity and reduced membrane permeability. In contrast, the most potent derivatives, such as β-sitosterol acetate, cholesterin, and carotene, exhibited markedly higher hydrophobicity (log P > 7), suggesting enhanced membrane permeation potential but diminished aqueous solubility. Additionally, compounds such as diphenyl sulfone and quinoline derivatives presented balanced physicochemical profiles with moderate logP and TPSA values, positioning them favorably within the drug-like chemical space. Quercetin-3-O-α-L-rhamnopyranoside, despite its strong docking affinity, demonstrated elevated TPSA (190.28 Å^2), which may limit passive permeability while contributing positively to solubility and target engagement. Overall, several derivatives displayed improved permeability profiles relative to the native ligand despite variations in solubility and molecular flexibility. Drug-like parameters further differentiated the structural suitability of the compounds, as shown in Table 3. The native ligand, although compliant with Lipinski's rule, failed to meet the Pfizer and Golden Triangle criteria, indicating potential limitations in early drug development. Conversely, diphenyl sulfone and 2,4-di-tert-butylphenol exhibited high QED scores (0.776 and 0.68, respectively), reflecting favorable medicinal chemistry attributes. Highly lipophilic triterpenoids, including β-sitosterol acetate and β-amyrone, showed moderate QED values because of their large size and sterol-like scaffolds, which inherently violate multiple rule-based filters.

Quercetin-3-O-α-L-rhamnopyranoside satisfied several drug-likeness criteria owing to its polyphenolic nature, but showed a high natural product (NP) score, consistent with its structural complexity. Collectively, the drug-likeness evaluation suggested that certain derivatives possess more promising pharmacological potential than the native ligand. The absorption predictions highlighted significant differences in the permeability and oral bioavailability, as presented in Table 4.

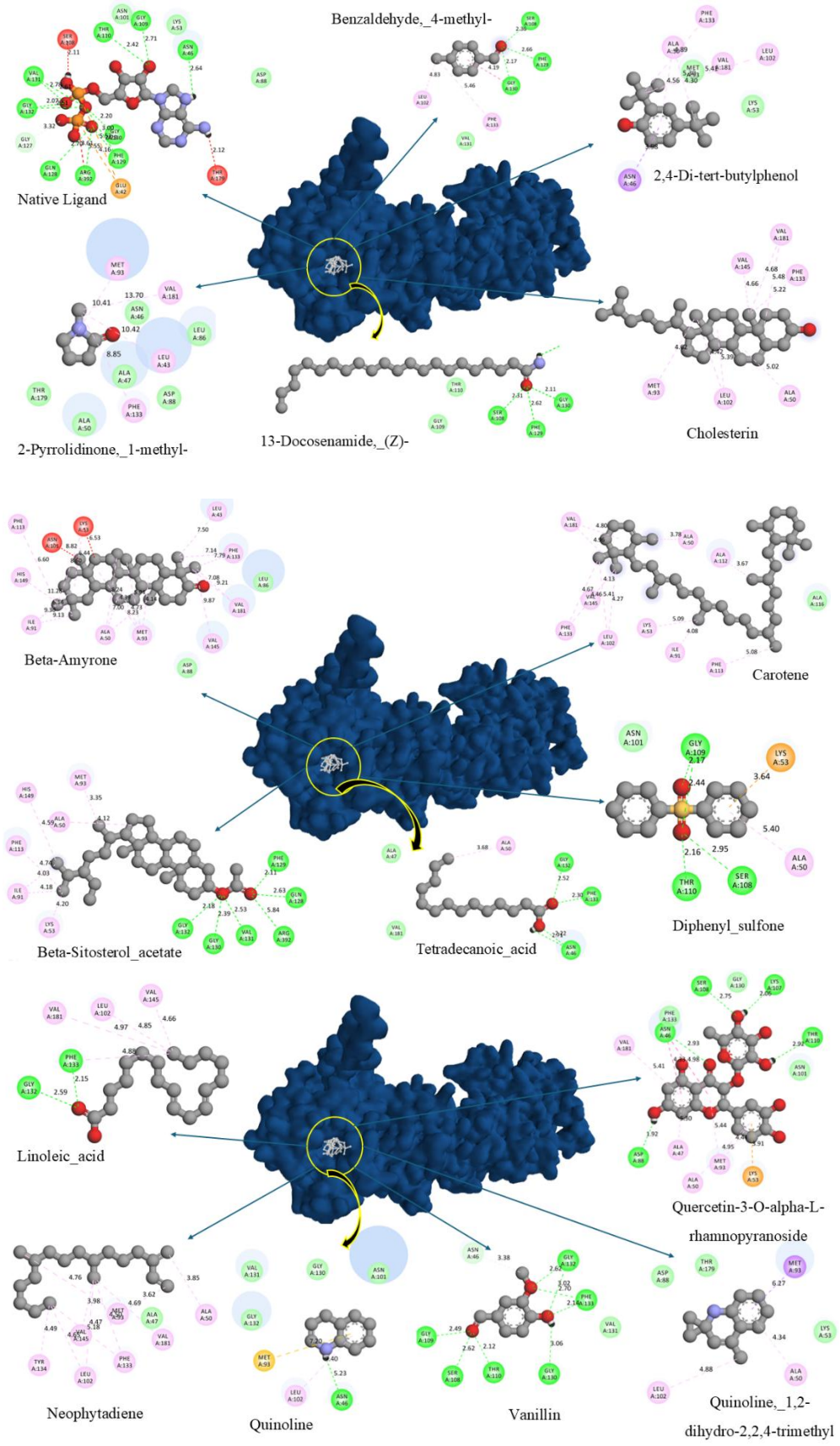

FIGURE 3 3D and 2D interactions of all selected compounds and native ligands with AhR (PDB ID: 7ZUB)

TABLE 2 Physicochemical evaluation of identified derivatives and native ligand

Compounds	MW	Volume	Dense	nHA	nHD	nRot	nRing	TPSA	logS	logP
Native ligand	427.03	327.842	1.30255	15	7	6	3	232.6	-1.9244	-2.67
2,4-Di-tert-butylphenol	206.17	243.025	0.84835	1	1	2	1	20.23	-4.2838	4.60654
B-Amyrone	424.37	488.171	0.86931	1	0	0	5	17.07	-6.8877	5.57527
B-Sitosterol acetate	456.4	522.814	0.87297	2	0	8	4	26.3	-8.2075	8.34632
Carotene	536.44	654.282	0.81989	0	0	10	2	0	-6.9345	7.17042
Cholesterin	386.35	447.476	0.8634	1	1	5	4	20.23	-6.7833	7.77015
Diphenyl sulfone	218.04	219.266	0.99441	2	0	2	2	34.14	-3.0395	2.27153
Quercetin-3-O-α-L-rhamnopyranoside	448.1	413.147	1.0846	11	7	3	4	190.28	-3.1327	1.31526
Quinoline, 1,2-dihydro-2,2,4-trimethyl	173.12	199.446	0.868	1	1	0	2	12.03	-3.4728	3.67097

The native ligand demonstrated moderate Caco-2 and MDCK permeability values and high human intestinal absorption (HIA = 0.949), indicating efficient absorption characteristics. In comparison, diphenyl sulfone, 2,4-di-tert-butylphenol, and the quinoline derivative exhibited improved permeability metrics, supporting a favorable absorption profile. Meanwhile, compounds such as carotene, cholesterol, and β-sitosterol acetate exhibited low predicted HIA due to their excessive hydrophobicity and larger molecular dimensions.

TABLE 3 Drug-likeness properties of designed derivatives

Compounds	QED	NP Score	Lipinski rule	Pfizer rule	GSK rule	Golden triangle	Chelator rule
Native ligand	0.281	1.388	1	0	1	0	1
2,4-Di-tert-butylphenol	0.68	-0.064	0	1	1	0	0
B-Amyrone	0.357	3.294	0	1	1	0	0
B-Sitosterol acetate	0.283	2.503	0	1	1	1	0
Carotene	0.192	1.829	1	1	1	1	0
Cholesterin	0.488	2.526	0	1	1	1	0
Diphenyl sulfone	0.776	-0.955	0	0	0	0	0
Quercetin-3-O-α-L-rhamnopyranoside	0.276	2.165	1	0	1	0	1
Quinoline, 1,2-dihydro-2,2,4-trimethyl	0.634	0.12	0	1	0	1	0

Despite limited permeability, quercetin-3-O-α-L-rhamnopyranoside display-ed excellent predicted oral bioavailability across the F20%, F30%, and F50% metrics (>0.99), suggesting its potential for significant systemic exposure following uptake. Relative to the native ligand, none of the derivatives outperformed all absorption parameters, although several demonstrated strengths in either permeability or bioavailability. Distribution analysis showed markedly higher plasma protein binding (PPB > 90%) for most derivatives than for the native ligand (24.44%), reflecting enhanced tissue distribution potential (Table 5).

In particular, β-amyrone, diphenyl sulfone, and quinoline derivatives exhibited PPB values exceeding 96%, which may prolong systemic retention, but could limit free drug availability. Blood–brain barrier (BBB) penetration was predicted to be minimal for quercetin-3-O-α-L-rhamnopyranoside, whereas several hydrophobic derivatives showed increased BBB permeability. The volume of distribution values was generally higher among the potent compounds, suggesting a widespread distribution beyond the vascular compartment. Metabolism predictions revealed various CYP450 interactions (Table 5). Lipophilic molecules, including β-sitosterol acetate and carotene, demonstrated strong substrate tendencies for CYP3A4 and CYP1A2, indicating potential metabolic clearance pathways. The native ligand showed comparatively fewer interactions across CYP isoforms, while quercetin-3-O-α-L-rhamnopyranoside exhibited limited inhibitory potential, suggesting a lower likelihood of metabolic drug–drug interactions. Excretion analysis revealed that potent derivatives generally exhibited higher clearance rates than the native ligand, with β-sitosterol acetate (10.51 mL/min/kg) and β-amyrone (9.28 mL/min/kg) demonstrating rapid elimination tendencies (Table 6).

Conversely, quercetin-3-O-α-L-rhamnopyranoside had the longest predicted half-life, indicating its potential for sustained therapeutic action. Regarding toxicity, the native ligand exhibited a higher carcinogenicity risk (0.7059), whereas most derivatives showed reduced carcinogenic potential. Compounds such as diphenyl sulfone and cholesterol demonstrated favorable safety profiles across multiple toxicity endpoints, although some derivatives exhibited elevated risks in specific categories, such as eye irritation or hepatotoxicity. Overall, several phytocompounds displayed improved toxicity margins compared to native ligand.

TABLE 4 Absorption properties of identified compounds

Compounds	Caco-2 Permeability	MDCK Permeability	Pgp-inhibitor	Pgp-substrate	HIA	F20%	F30%	F50%
Native Ligand	-5.8725	-5.1624	2.47E-06	7.54E-06	0.94944	0.03533	0.99336	0.87572
2,4-Di-tert-butylphenol	-4.896	-4.6724	0.97166	0.26444	0.29008	0.90523	0.84129	0.99137
B-Amyrone	-5.0686	-4.8299	0.99444	0.00011	1.29E-05	0.08834	0.03701	0.95267
B-Sitosterol acetate	-5.1101	-5.0352	0.007	0.00822	1.68E-05	0.01736	0.53544	0.99667
Carotene	-4.8965	-4.7313	0.97546	0.51102	1.91E-06	0.00388	0.07258	0.99588
Cholesterin	-5.2244	-5.0866	8.06E-05	0.07422	9.54E-07	0.00055	0.135	0.9826
Diphenyl sulfone	-4.4929	-4.5741	0.98697	0.00445	1.19E-07	0.00016	0.01176	0.00059
Quercetin-3-O-α-L-rhamnopyranoside	-6.0447	-4.978	1.23E-05	0.27949	0.10505	0.65736	0.9985	0.99987
Quinoline, 1,2-dihydro-2,2,4-trimethyl	-4.7987	-4.6083	0.5403	0.93933	0.00078	0.0405	0.12576	0.49223

TABLE 5 Distribution and metabolism parameter of selected molecules

Compounds	Distribution				Metabolism									
	PPB%	VD	BBB	Fu	Inhibitor	Substrate	Inhibitor	Substrate	Inhibitor	Substrate	Inhibitor	Substrate	Inhibitor	Substrate
Native Ligand	24.4391	-0.4418	0.00651	62.155	7.60E-18	3.04E-23	4.71E-18	9.24E-18	3.08E-11	0.24632	5.29E-09	1.14E-11	2.10E-11	3.19E-11
2,4-Di-tert-butylphenol	95.1301	0.29754	0.00244	3.68719	0.88468	0.00561	0.82044	0.03017	0.08209	0.1131	0.01221	0.09306	0.02091	0.84027
B-Amyrone	97.7827	0.4243	0.88068	2.61269	4.18E-07	0.99997	0.03338	1	0.09905	0.03342	1.13E-05	1.68E-05	0.06163	0.99999
B-Sitosterol acetate	91.9372	-0.1641	0.01841	8.44961	1.52E-05	0.00027	0.42962	0.99983	0.27947	1.77E-05	0.01469	0.00457	0.28187	1
Carotene	95.1475	0.56702	2.68E-08	5.05392	0.03963	1	1	1	0.81624	1	0.72501	0.99976	0.99699	0.99948
Cholesterin	84.8103	-0.1666	0.35119	13.4594	7.46E-07	3.41E-08	0.01185	0.00412	0.03016	4.30E-08	0.10938	0.00016	0.31158	0.99992
Diphenyl sulfone	96.8116	-0.243	0.89251	2.44156	0.19357	0.09065	0.93084	0.79413	0.92628	0.75988	0.05128	0.0127	0.26537	0.9823
Quercetin-3-O-α-L-rhamnopyranoside	86.137	-0.0638	0.00014	12.8877	0.26199	0.03064	2.07E-05	3.19E-05	0.00016	0.0025	0.00064	0.0066	0.93583	1.17E-06
Quinoline, 1,2-dihydro-2,2,4-trimethyl	98.6889	0.37804	0.75335	1.39741	0.99964	0.90393	0.99934	0.99998	0.99928	0.99929	0.99607	0.89877	0.93656	0.5829

Environmental toxicity assessment revealed that the native ligand exhibited minimal bioaccumulation potential (BCF = 0.0167), which was significantly lower than that of all the tested derivatives (Table 7). Lipophilic derivatives, such as carotene, β-sitosterol acetate, and cholesterol, showed higher BCF values, indicative of environmental persistence. However, the LC_{50} (fish and Daphnia) values for these compounds were also relatively high, implying lower acute aquatic toxicity. Diphenyl sulfone and quercetin-3-O-α-L-rhamnopyranoside demonstrated moderate environmental safety, which is consistent with their balanced physicochemical profiles. Compared with the native ligand, most derivatives exhibited slightly increased environmental

bioaccumulation, but remained within acceptable ecological toxicity thresholds.

TABLE 6 Excretion and toxicity properties of identified compounds and native ligand

Compounds	Excretion			Toxicity								
	CL-plasma	T1/2	H-HT	DILI	Ames toxicity	Rat Oral Acute toxicity	FDAMDD	Skin sensitization	Carcinogenicity	Eye corrosion	Eye irritation	Respiratory toxicity
Native ligand	1.96411	2.11991	0.12705	0.98012	0.11964	0.03693	0.9902	0.99348	0.7059	0.00058	0.70142	0.98953
2,4-Di-tert-butylphenol	7.75242	0.49347	0.24323	0.12496	0.10042	0.40366	0.59979	0.62457	0.24473	0.94682	0.99461	0.76859
B-Amyrone	9.28657	0.09583	0.68022	0.48852	0.29252	0.55836	0.54479	0.79817	0.89586	0.19953	0.65313	0.74048
B-Sitosterol acetate	10.5163	0.25843	0.48888	0.44335	0.2158	0.16895	0.52948	0.98651	0.70561	0.44801	0.87943	0.84478
Carotene	9.08082	0.28143	0.45691	0.28453	0.28837	0.69269	0.8312	0.69955	0.73821	0.00183	0.26382	0.688
Cholesterin	13.185	0.5496	0.55548	0.19952	0.21351	0.1162	0.58606	0.93147	0.8646	0.59201	0.97123	0.72158
Diphenyl sulfone	3.32934	1.36043	0.89057	0.99399	0.03528	0.06179	0.07751	0.41561	0.1683	0.64822	0.99222	0.03165
Quercetin-3-O-α-L-rhamnopyranoside	3.60166	3.72033	0.43791	0.92884	0.7506	0.20331	0.37263	0.99671	0.10018	0.00391	0.98316	0.28876
Quinoline, 1,2-dihydro-2,2,4-trimethyl	8.69177	0.38757	0.65227	0.52667	0.50997	0.37735	0.33919	0.66066	0.72197	0.55763	0.97729	0.67588

The ADMET radars of the identified derivatives are listed in Figure 4. The integrated ADMET assessment demonstrated that the selected phytocompounds possessed diverse pharmacokinetic and safety profiles, with several outperforming the native ligand in critical categories, such as drug-likeness, toxicity, metabolic stability, and distribution. Quercetin-3-O-α-L-rhamnopyranoside, diphenyl sulfone, and quinoline derivatives were the most balanced candidates, offering an optimal blend of predicted solubility, bioavailability, safety, and metabolic compatibility. Collectively, these findings underscore the therapeutic relevance of *Cissus quadrangularis* constituents as potential AhR modulators and warrant further experimental validation.

TABLE 7 Environmental toxicity properties of most potent compounds and native ligand

Compounds	BCF	IGC50	LC50FM	LC50DM
Native ligand	0.0167	2.36705	3.40548	3.76102
2,4-Di-tert-butylphenol	2.7751	4.7323	5.77449	6.11945
B-Amyrone	2.92973	4.68152	5.44929	5.3017
B-Sitosterol acetate	3.11672	4.91379	5.72878	5.29947
Carotene	4.10241	5.69372	8.13336	7.13627
Cholesterin	3.08619	4.73005	5.42622	5.21836
Diphenyl sulfone	0.65058	3.29799	3.6132	3.81358
Quercetin-3-O-α-L-rhamnopyranoside	0.83096	3.52122	4.08883	4.6393
Quinoline, 1,2-dihydro-2,2,4-trimethyl	2.14762	3.55932	4.11826	4.26451

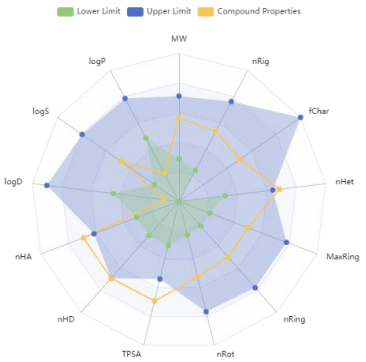

Native Ligand

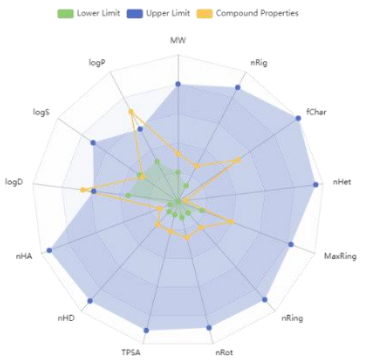

2,4-Di-tert-butylphenol

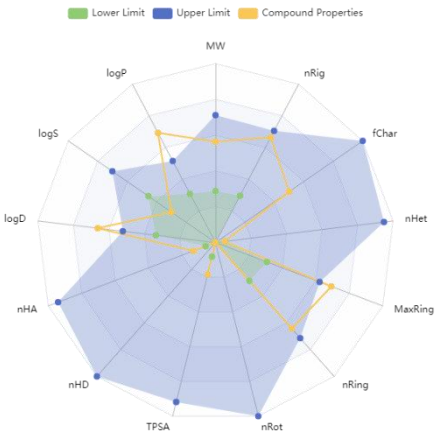

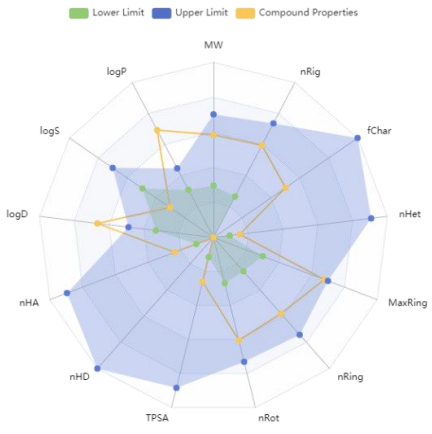

B-Sitosterol acetate

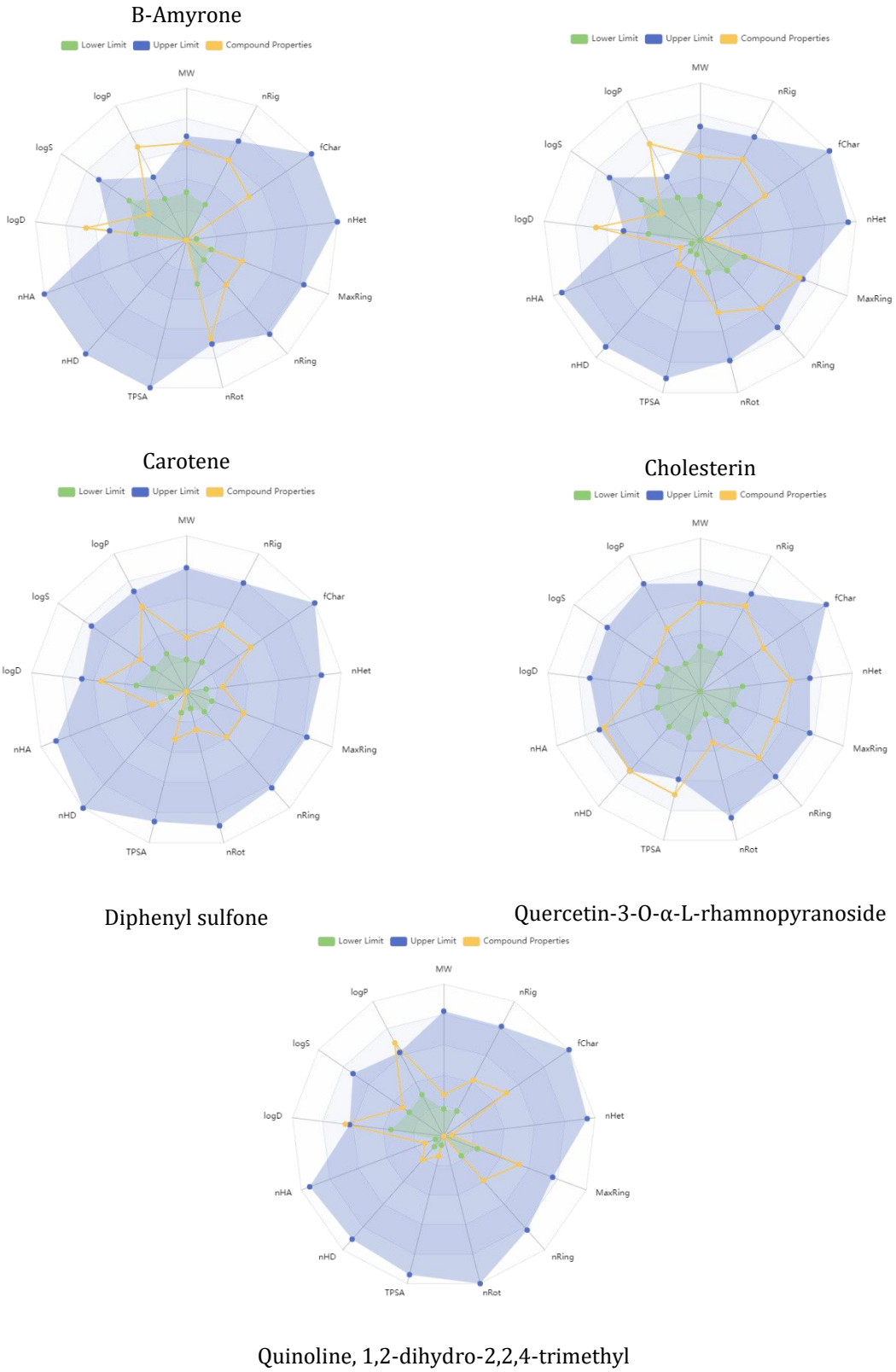

FIGURE 4 ADMET radar of most potent compounds and native ligand

Conclusion

The present study provides a comprehensive computational investigation of phytoconstituents from *Cissus quadrangularis* as potential modulators of AhR, a therapeutic target implicated in psoriasis. Molecular docking analysis revealed that several

compounds exhibited strong and favorable binding interactions with AhR, surpassing the affinity and stability of the native ligand. Among them, quercetin-3-O-α-L-rhamnopyranoside, β-sitosterol acetate, cholesterol, and β-amyrone have emerged as the most potent candidates, demonstrating extensive hydrogen bonding, π-interactions, and hydrophobic stabilization within the active site of the receptor. Based on these findings, ADMET profiling was performed to assess the pharmacokinetic suitability and safety of the top-performing molecules. Several derivatives exhibited improved drug-likeness, favorable permeability indices, acceptable metabolic stability, and lower predicted carcinogenicity than the native ligand. Quercetin-3-O-α-L-rhamnopyranoside and diphenyl sulfone displayed particularly balanced ADMET characteristics, whereas triterpenoid compounds showed enhanced lipophilicity and distribution potential. Environmental toxicity assessments further supported the safety profiles of most phytochemicals. Overall, integrated docking and ADMET analyses indicated that these phytoconstituents, particularly quercetin-3-O-α-L-rhamno-pyranoside, β-sitosterol acetate, and β-amyrone, hold strong promise as AhR modulators and warrant further experimental validation for the development of novel psoriasis therapeutics. Nevertheless, further *in vitro* and *in vivo* experimental investigations are essential to validate the predicted AhR-modulatory activity, pharmacokinetic behavior, and therapeutic efficacy of these lead phytoconstituents before their translation to clinical application in psoriasis management

ORCID

Konatham Teja Kumar Reddy
https://orcid.org/0000-0002-0227-2248
Mobeen Shaik
https://orcid.org/0000-0002-8644-7617
Karthickeyan Krishnan
https://orcid.org/0000-0002-8644-7617
Phanindra Erukulla
https://orcid.org/0009-0001-2900-2881
Pericharla Venkata Narasimha Raju
https://orcid.org/0009-0003-2259-6693
T. Siva Krishna
https://orcid.org/0000-0001-5408-8341
Mohit Kumar
https://orcid.org/0009-0001-8236-7396
CH K V L S N Anjana Male
https://orcid.org/0009-0001-8236-7396

Authors' Contributions

Conceptualization; Data curation; Formal analysis; Investigation; Methodology; Project administration; Resources; Software; Supervision; Validation; Visualization; Writing original draft; Writing review and editing by All Authors are contributed equally.

References

[1] Raharja, A., Mahil, S.K., Barker, J.N. Psoriasis: A brief overview. *Clinical Medicine*, **2021**, 21(3), 170-173.
[2] Rendon, A., Schäkel, K. Psoriasis pathogenesis and treatment. *International Journal of Molecular Sciences*, **2019**, 20(6), 1475.
[3] Sieminska, I., Pieniawska, M., Grzywa, T.M. The immunology of psoriasis—current concepts in pathogenesis. *Clinical Reviews in Allergy & Immunology*, **2024**, 66(2), 164-191.
[4] Yamazaki, F. Psoriasis: Comorbidities. *The Journal of Dermatology*, **2021**, 48(6), 732-740.
[5] Dawe, H.R., Di Meglio, P. The aryl hydrocarbon receptor (ahr): Peacekeeper of the skin. *International Journal of Molecular Sciences*, **2025**, 26(4), 1618.
[6] Li, Y., Zeng, Y., Chen, Z., Tan, X., Mei, X., Wu, Z. The role of aryl hydrocarbon receptor in vitiligo: A review. *Frontiers in Immunology*, **2024**, 15, 1291556.
[7] Silverberg, J.I., Boguniewicz, M., Quintana, F.J., Clark, R.A., Gross, L., Hirano, I., Tallman, A.M., Brown, P.M., Fredericks, D., Rubenstein, D.S. Tapinarof validates the aryl hydrocarbon receptor as a therapeutic target: A clinical review. *Journal of Allergy and Clinical Immunology*, **2024**, 154(1), 1-10.
[8] Bahman, F., Choudhry, K., Al-Rashed, F., Al-Mulla, F., Sindhu, S., Ahmad, R. Aryl hydrocarbon receptor: Current perspectives on key signaling

partners and immunoregulatory role in inflammatory diseases. *Frontiers in Immunology*, **2024**, 15, 1421346.
[9] Barroso, A., Mahler, J.V., Fonseca-Castro, P.H., Quintana, F.J. The aryl hydrocarbon receptor and the gut–brain axis. *Cellular & Molecular Immunology*, **2021**, 18(2), 259-268.
[10] Pal, I., Singh, V., Naicker, A., Palmer, K. Product development with *Cissus quadrangularis* (hadjod) to create awareness among young adults. *South African Journal of Botany*, **2024**, 171, 719-725.
[11] Dhanasekaran, S. Phytochemical characteristics of aerial part of *Cissus quadrangularis* (l) and its in-vitro inhibitory activity against leukemic cells and antioxidant properties. *Saudi Journal of Biological Sciences*, **2020**, 27(5), 1302-1309.
[12] Kaur, J., Dhiman, V., Bhadada, S., Katare, O., Ghoshal, G. LC/MS guided identification of metabolites of different extracts of *Cissus quadrangularis*. *Food Chemistry Advances*, **2022**, 1, 100084.
[13] Garg, J., Ghoshal, G., Bhadada, S.K., Katare, O.P. Derivatisation mechanistic-guided identification of phytoconstituents of different extracts of *Cissus quadrangularis* by tlc and standardization by hptlc. *Phytomedicine Plus*, **2024**, 4(3), 100601.
[14] Jadhav, S., Dighe, P. In vitro evaluation, and molecular docking studies of novel pyrazoline derivatives as promising bioactive molecules. *Journal of Pharmaceutical Sciences and Computational Chemistry*, **2025**, 1(3), 190-209.
[15] Halder, D., Das, S. Molecular docking and dynamics based approach for the identification of kinase inhibitors targeting PI3KA against non-small cell lung cancer: A computational study. *RSC Advances*, **2022**, 12(33), 21452-21467.
[16] Anaridha, S., PK, M.I., Meeran, S., Shabeer, T. Computational analysis using admet profiling, dft calculations and molecular docking of two anti-cancer drugs. *Turkish Computational and Theoretical Chemistry*, **2023**, 7(1), 37-50.
[17] Boulaamane, Y., Touati, I., Qamar, I., Ahmad, I., Patel, H., Chandra, A., Britel, M.R., Maurady, A. In silico discovery of dual ligands targeting mao-b and aa2ar from african natural products using pharmacophore modelling, molecular docking, and molecular dynamics simulations. *Chemistry Africa*, **2024**, 7(8), 4337-4359.
[18] Stockinger, B., Meglio, P.D., Gialitakis, M., Duarte, J.H., The aryl hydrocarbon receptor: Multitasking in the immune system. *Annual Review of Immunology*, **2014**, 32(1), 403-432.
[19] Murray, I.A., Patterson, A.D., Perdew, G.H. Aryl hydrocarbon receptor ligands in cancer: Friend and foe. *Nature Reviews Cancer*, **2014**, 14(12), 801-814.
[20] Quintana, F.J., Sherr, D.H. Aryl hydrocarbon receptor control of adaptive immunity. *Pharmacological Reviews*, **2013**, 65(4), 1148-1161.
[21] Zhao, X., Wang, Y., Zhang, Z., Velu, P., Liu, R. In-vitro antioxidant, in-vitro and in-silico ovarian anticancer activity (ovarian cancer cells-pa1) and phytochemical analysis of *Cissus quadrangularis* l. Ethanolic extract. *Combinatorial Chemistry & High Throughput Screening*, **2024**, 27(10), 1504-1512.
[22] Sivapria, A.S., Kariyil, B.J., Menon, P. In silico screening of phytoconstituents of *Cissus quadrangularis* and chromolaena odorata against proteins of antimicrobial resistance and wound healing. *Plant Science Today*, **2024**, 11(1), 531–43.
[23] Khan, S.L., Bakshi, V. LC-HRMS and *In Silico* Analysis of Ailanthus excelsa Metabolites Targeting EGFR Triple Mutation (L858R/T790M/C797S), *Advanced Journal of Chemistry, Section A*. **2026**, 9(2), 292-311.
[24] Prathyusha, S., Shankar Gupta, P., Kumar, A.K., Hussain Syed, S., Shaik, M., Jahnavi, P., Rani, S., Rajashakar, V. Theoretical and computational study of bioactive compounds from myrica nagi as inhibitors of neuroendocrine and opioid receptors: A molecular docking and dynamics approach. *Advanced Journal of Chemistry Section A*, **2026**, 9(2), 223–42.
[25]Kale, M., Wayal, S. Molecular docking, synthesis and biological screening of some novel benzothiazoles as acetylcholinesterase inhibitors. *Advanced Journal of Chemistry Section A*, **2026**, 9(2), 208–22.
[26] Tamboli, A., Tayade, S. In-depth investigation of berberine and tropane through computational screening as possible dpp-iv inhibitors for the treatment of t2dm. *Journal of Pharmaceutical Sciences and Computational Chemistry*, **2025**, 1(1), 1-11.
[27] Boutalaka, M., El Bahi, S., Alaqarbeh, M., El Alaouy, M.A., Koubi, Y., Khatabi, K.E., Maghat, H., Bouachrine, M., Lakhlifi, T. Computational investigation of imidazo [2, 1-b] oxazole derivatives as potential mutant braf kinase inhibitors: 3D-QSAR, molecular docking, molecular dynamics simulation, and ADMETox studies. *Journal of*

Biomolecular Structure and Dynamics, **2024**, 42(10), 5268-5287.
[28] Sabale, K.P., Kakade, G.K. Silico screening of *N*-ethylidene-4- (furan-2-yl) oxazol-2-amine derivatives by computational analysis as potential murg- glycosyltransferase inhibitors for bacterial infection. *Advanced Biomedical*, **2025**, 16, 66–85.

How to cite this article: Konatham Teja Kumar Reddy, Mobeen Shaik, Karthickeyan Krishnan, Phanindra Erukulla, Pericharla Venkata Narasimha Raju, T. Siva Krishna, Mohit Kumar, CH K V L S N Anjana Male, Computational investigation of *Cissus quadrangularis* phytoconstituents as aryl hydrocarbon receptor modulators for psoriasis therapy. *Journal of Medicinal and Pharmaceutical Chemistry Research*, 2026, 8(9), 2255-2275 **Link:** https://jmpcr.samipubco.com/article_240263.html